Original Article

Identification and *in vitro* validation of diagnostic and prognostic biomarkers for lung squamous cell carcinoma

Xiaopeng Zhao[1], Chong Yuan[2], Xu He[1], Miao Wang[1], Haoran Zhang[1], Jingge Cheng[1], Hongyan Wang[1]

[1]Department of Thoracic Surgery, The Fourth Hospital of Hebei Medical University, Shijiazhuang, China; [2]The First Outpatient Department Directly Under Hebei Province, Shijiazhuang, China

Contributions: (I) Conception and design: H Wang, X Zhao; (II) Administrative support: H Wang; (III) Provision of study materials or patients: C Yuan, X He, M Wang; (IV) Collection and assembly of data: X He, M Wang; (V) Data analysis and interpretation: H Zhang, J Cheng; (VI) Manuscript writing: All authors; (VII) Final approval of manuscript: All authors.

Correspondence to: Hongyan Wang, MD. Department of Thoracic Surgery, The Fourth Hospital of Hebei Medical University, No. 12, JianKang Road, Shijiazhuang, China. Email: tiger-wt@hotmail.com.

Background: The aim of the present study was to find diagnostic and prognostic biomarkers for lung squamous cell carcinoma (LUSC) and to validate key biomarkers *in vitro*.

Methods: RNA sequencing was used to identify differentially expressed mRNAs (DEmRNAs) and differentially expressed long non-coding RNAs (DElncRNAs) in LUSC tissues. RNA sequencing results were validated using a published dataset. Diagnostic and prognostic values of candidate genes were evaluated by receiver-operating characteristic (ROC) curve analysis and survival analysis, respectively. To determine the effect of *MIR205HG* in LUSC, *MIR205HG* expression was knocked down in NCI-H520 cells. 3-(4,5-dimethylthiazol-2-yl)-2,5-diphenyltetrazolium bromide (MTT) assay and Transwell assay were used to respectively detect the effect of *MIR205HG* on cell proliferation and migration.

Results: In total, 1,946 DEmRNAs and 428 DElncRNAs were identified in LUSC compared with normal tissues. A total of 851 DElncRNA-DEmRNA co-expression pairs were obtained. With the exception of *NEAT1*, *MCM2*, *SERPINB5*, *ITGB8*, *CASC19*, and *MIR205HG* were upregulated in LUSC. ROC curve analysis indicated that *MCM2*, *SERPINB5*, *ITGB8*, *CASC19*, and *MIR205HG* could predict LUSC. Survival analysis suggested that *SERPINB5*, *NEAT1*, and *MIR205HG* had potential prognostic value for LUSC. *MIR205HG* knockdown inhibited cell proliferation and migration, and significantly reduced the expression of *ITGB8*.

Conclusions: The findings of the present study could help determine the pathogenesis of LUSC and provide new and accurate therapeutic targets for its treatment.

Keywords: Lung squamous cell carcinoma (LUSC); RNA sequencing; differentially expressed mRNAs (DEmRNAs); differentially expressed long non-coding RNAs (DElncRNAs); co-expression

Submitted Mar 02, 2022. Accepted for publication Apr 08, 2022.
doi: 10.21037/jtd-22-343
View this article at: https://dx.doi.org/10.21037/jtd-22-343

Introduction

Lung cancer is one the most commonly diagnosed malignancies and is the leader cause of cancer-related morbidity globally (1). Non-small cell lung cancer is the major subtype of lung cancer. Lung squamous cell carcinoma (LUSC) is a most frequent subtype of non-small cell lung cancer and accounts for approximately 40% of diagnosed cases of lung cancer each year (2). Currently, the main treatment strategies for LUSC include surgery, radiotherapy, and chemotherapy (3). However, the 5-year overall survival rate for LUSC patients remains poor, largely due to limited understanding of the molecular mechanisms of LUSC in published studies (4,5). Therefore,

it is important to find effective and promising biomarkers for LUSC patients.

Long non-coding RNAs (lncRNAs), which are defined as RNAs with more than 200 nucleotides, have been the focus of increasing attention and have been widely associated with multiple diseases, such as colorectal cancer and Alzheimer's disease (6,7). With the emergence of sequencing technology, bioinformatics have become the most frequently used method to investigate the pathological mechanism of various diseases (8,9). For example, Kim *et al.* reported the comprehensive single-cell transcriptome profiling of lung adenocarcinoma from early to advanced stages of primary cancer and distant metastases, and unveiled cellular dynamics and molecular features associated with the tumor progression (10). However, this atlas has just revealed the characteristics of tumor cells and associated microenvironments. Some changes of molecular networks during tumor progression have not been studied in lung cancer, especially in LUSC.

Interestingly, more and more studies have found that lncRNA dysregulation is associated with the occurrence and progression of a variety of cancers (9,11). Until now, the function of lncRNAs in the pathogenesis of LUSC has not been determined in depth. Therefore, it is important to expand our understanding of the pathogenesis of LUSC and to screen novel biomarkers to improve LUSC treatment strategies. In the present study, we applied RNA sequencing to differentially expressed mRNA (DEmRNAs) and differentially expressed lncRNAs (DElncRNAs) in LUSC patients versus controls. Moreover, functional annotation and the protein-protein interaction (PPI) network of DEmRNAs were used. DEmRNA-DElncRNA interaction analysis and functional annotation of DEmRNAs co-expressed with DElncRNAs were also used, and the diagnostic and prognostic values of candidate genes were evaluated. The aim of the present study was to determine the underlying mechanisms of LUSC and find novel and accurate biomarkers. We present the following article in accordance with the STARD and MDAR reporting checklists (available at https://jtd.amegroups.com/article/view/10.21037/jtd-22-343/rc).

Methods

Patients

Three LUSC patients were included in this study. Six tissue samples (3 LUSC tumor samples and 3 paired adjacent normal tissue samples) were used for RNA sequencing. All patients provided signed informed consent. The present study was approved by the ethics committee of the Fourth Hospital of Hebei Medical University (No. 2019KY256). The study was conducted in accordance with the Declaration of Helsinki (as revised in 2013).

RNA isolation and sequencing

Total RNA was extracted from samples using the TRIzol kit (Invitrogen, Carlsbad, CA, USA). Total RNA was further purified with the Ribo-Zero Magnetic kit (EpiCentre, Madison, WI, USA). Illumina Hiseq Xten platform (Illumina, San Diego, CA, USA) was used to conduct mRNA sequencing. The lncRNA and mRNA expression levels were compared using edgeR (https://www.bioconductor.org/packages/release/bioc/html/edgeR.html) (12). MRNAs and lncRNAs with |log2fold change (FC)| >1 and $P<0.05$ were defined as significant DEmRNAs and DElncRNAs. Volcano plot was generated in R package (https://www.r-project.org/). Hierarchical clustering analysis of top 100 DEmRNAs and DElncRNAs was structured by heatmap.2 (13).

Functional annotation

Gene Ontology (GO) classification and Kyoto Encyclopedia of Genes and Genomes (KEGG) pathway enrichment analysis was done via GeneCoDis3 (14). Significant enrichment was defined as $P<0.05$.

PPI network construction

The top 50 upregulated and downregulated DEmRNAs were used to establish the PPI network using BioGRID and Cytoscape 3.6.1 (https://cytoscape.org/). Node and edge represented the protein and interaction between two proteins, respectively.

DEmRNA-DElncRNA interaction analysis

To analyze DEmRNAs of DElncRNAs with cis-regulatory effects, DEmRNAs transcribed within a 100 kb window upstream or downstream of DElncRNAs between LUSC and controls were obtained. DEmRNAs co-expressed with DElncRNAs were also screened, and pairwise Pearson correlation coefficients between DEmRNAs and DElncRNAs were analyzed. DElncRNA-DEmRNA pairs with $P<0.001$ and $r\geq0.999$ served as significant mRNA-lncRNA co-expression pairs.

Validation in The Cancer Genome Atlas (TCGA) dataset

The expression pattern of selected DEmRNAs and DElncRNAs was validated in TCGA dataset. TCGA dataset consisted of 501 patients with LUSC and 49 controls.

Receiver-operating characteristic (ROC) curve analyses

To evaluate the diagnostic value of DEmRNAs and DElncRNAs in LUSC, the pROC package (15) was use to generate ROC curves, and the area under the ROC curve (AUC) represented the diagnostic value. When the AUC value was >0.8, DEmRNA/DElncRNA was considered to be able to distinguish between cases and controls with good specificity and sensitivity.

Survival analysis

To evaluate the prognostic biomarkers of candidate genes, survival analysis was generated using clinical data from TCGA dataset. Kaplan-Meier curve was plotted using survival curves (https://cran.r-project.org/web/packages/survival/index.html) in R package.

Cell culture and transfection

Human LUSC cell lines (NCI-H520) were obtained from American Type Culture Collection (Manassas, VA, USA) and cultured in endothelial cell growth medium (Gibco, Rockville, MD, USA) supplemented with 10% fetal bovine serum (FBS) (Gibco) in 5% CO_2 at 37 ℃. Small interfering RNA targeting MIR205HG and scramble siRNA of *MIR205HG* [normal control (NC)] was purchased from Guangzhou Ribobio (Guangzhou, China). For cell transfection, NCI-H520 cells were inoculated with 60–70% cell density and allowed to adhere overnight. The corresponding plasmid was then transfected into cells by Lipofectamine 2000 (Gibco) according to the manufacturer's instructions. After 48 h, cells were collected for subsequent experiments.

Cell Counting Kit-8 (CCK-8)

Cell viability was measured using the CCK-8 kit. Briefly, treated NCI-H520 cells were inoculated on 96-well plates for 12 h, and 10 μL of CCK-8 reagent was added to each well at 37 ℃ for 4 h. The absorbance value of each well at 450 nm was determined using a microplate reader.

Transwell assay

Cell migration capacities were detected using Transwell assays. Cells resuspended in serum-free medium were placed into the upper chamber of a 24-Transwell plate with an 8-μm pore filter (BD Biosciences, Franklin Lakes, NJ, USA). Then, 500 μL of growth medium containing 10% FBS was added to the lower chamber. After incubation for 24 h, cells that moved through the underside of the membrane filter were fixed with 4% paraformaldehyde and stained with 0.25% crystal violet. The number of migrated or invaded cells was counted, and the images were photographed under a light microscope (Olympus, Tokyo, Japan).

Quantitative reverse transcription polymerase chain reaction (qRT-PCR)

Total RNA was isolated from NCI-H520 cells using a RNA simple total RNA kit (Tiangen, Beijing, China) and then reverse transcribed with the Fast Quant RT (Tiangen) according to the manufacturer's instructions. QRT-PCR was performed using Super Real PreMix Plus SYBR Green (Tiangen) on a QuantStudio 6 Flex system (Thermo Fisher). The sequences of forward and reverse primers for all of the genes analyzed were as follows: *MIR205HG* (forward: ATCTCTCAAGTACCCATCTTGGA; reverse: GGCCTCATGGTTGTCAGCTC) and *ITGB8* (forward: CGTGACTTTCGTCTTGGATTTGG; reverse: TCCTTTCGGGGTGGATGCTAA). The relative quantification of genes was calculated using $2^{-\Delta\Delta Ct}$ method.

Statistical analysis

The lncRNA and mRNA expression levels were compared using edgeR (https://www.bioconductor.org/packages/release/bioc/html/edgeR.html). Pairwise Pearson correlation coefficients between DEmRNAs and DElncRNAs were analyzed. Wilcoxon test was used to analyze the expression difference of DEmRNAs and DElncRNAs between groups in TCGA dataset. The *t*-test was used for expression difference analysis of DEmRNAs and DElncRNAs in qRT-PCR.

Results

DEmRNAs and DElncRNAs in LUSC

Based on the thresholds of $|\log2FC| > 1$ and $P<0.05$, a total of 1,946 (940 downregulated and 1,006 upregulated)

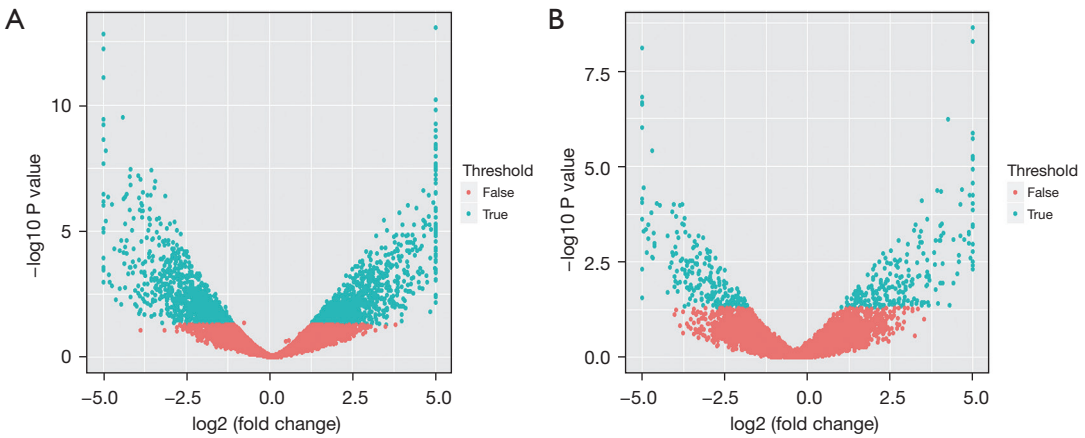

Figure 1 Volcano plot of (A) DEmRNAs and (B) DElncRNAs. DEmRNAs, differentially expressed mRNAs; DElncRNAs, differentially expressed long non-coding RNAs.

DEmRNAs and 428 (206 downregulated and 222 upregulated) DElncRNAs were obtained in LUSC. As shown in *Figure 1*, the volcano plot shows the overall distribution of DEmRNAs and DElncRNAs. Hierarchical clustering analysis of the top 100 DEmRNAs and DElncRNAs is shown in *Figure 2A*,*2B*, respectively. Circus plots represent the distribution of DElncRNAs and DEmRNAs on chromosomes (*Figure 2C*).

Functional annotation of DEmRNAs

GO and KEGG enrichment analyses were used to determine the biological function of DEmRNAs. GO enrichment analysis results revealed that these DEmRNAs were significantly enriched in mitotic cell cycle (P=1.54E-31), cell adhesion (P=2.71E-31), cytoplasm (P=2.19E-84), protein binding (P=9.16E-83), and nucleotide binding (P=4.84E-37) (*Figure 3A-3C*). Through KEGG enrichment analysis, cell cycle (P=8.23E-17), cancer pathways (P=8.41E-12), the p53 signaling pathway (P=9.51E-10), extracellular matrix (ECM)-receptor interaction (P=9.75E-09), DNA replication (P=1.11E-08), and the mitogen-activated protein kinase (MAPK) signaling pathway (P=1.47E-08) were found to be significantly enriched pathways (*Figure 3D*).

PPI network

The PPI network of the top 50 upregulated and downregulated DEmRNAs consisted of 255 nodes and 253 edges (*Figure 4*). *TP63* (degree =21), *TRIM29* (degree =15), *FOS* (degree =13), *MCM2* (degree =12), *LRRK2* (degree =11), *NR4A1* (degree =9), *HIST2H3C* (degree =9), *CALML3* (degree =8), *HBB* (degree =7), *PKP1* (degree =7), and *SERPINB5* (degree =7) were considered hub proteins.

DEmRNA-DElncRNA interaction analysis and functional annotation of DEmRNAs co-expressed with DElncRNAs

A total of 851 DElncRNA-DEmRNA co-expression pairs (such as *MIR205HG-ITGB8*), including 213 DElncRNAs and 377 DEmRNAs, were identified with r<0.999 and P<0.01 (*Figure 5*). GO enrichment analysis results revealed that these DEmRNAs were significantly enriched in cellular response to hypoxia (P=2.82E-09), cell adhesion (P=6.18E-08), plasma membrane (P=3.02E-16), protein binding (P=1.27E-18), and receptor binding (P=9.98E-09) (*Figure 6A-6C*). Based on the KEGG enrichment analysis, cell cycle (P=3.57E-05), cell adhesion molecules (P=4.00E-05), the p53 signaling pathway (P=5.71E-04), ECM-receptor interaction (P=1.59E-03), small cell lung cancer (P=1.59E-03), and focal adhesion (P=3.89E-03) were significantly enriched pathways (*Figure 6D*).

TCGA dataset validation

The expression patterns of 3 DEmRNAs (*MCM2*, *SERPINB5*, and *ITGB8*) and 3 DElncRNAs (*NEAT1*, *CASC19*, and *MIR205HG*) were validated in LUSC. As shown in *Figure 7*, *NEAT1* was downregulated, which was inconsistent with our RNA sequencing results. *MCM2*, *SERPINB5*, *ITGB8*, *CASC19*, and *MIR205HG* were upregulated in LUSC, which was consistent with our RNA sequencing results.

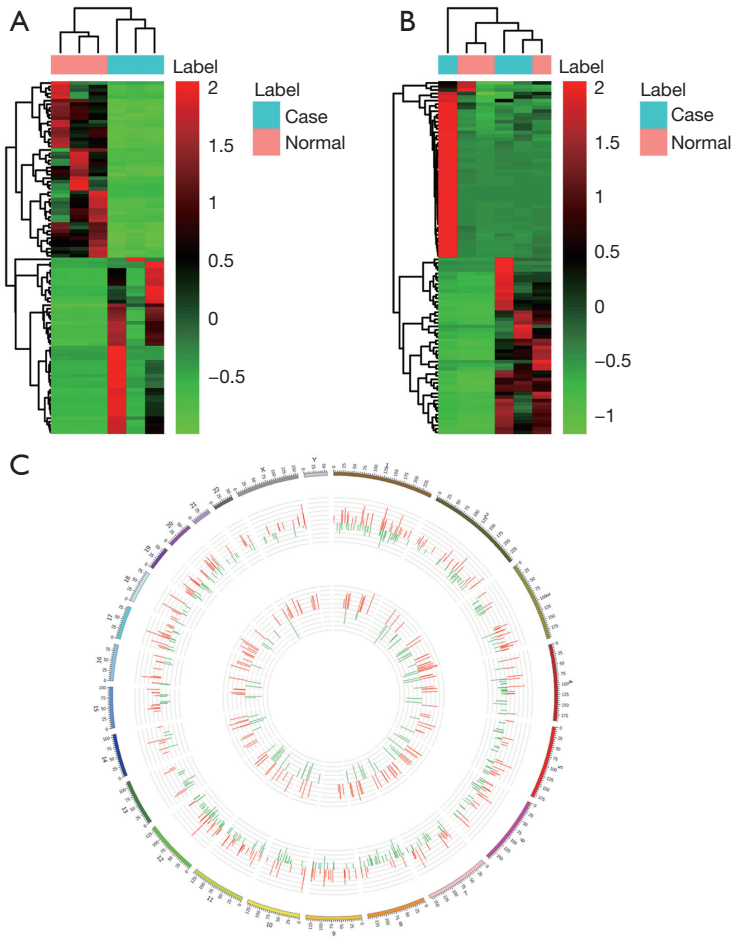

Figure 2 Heat map and Circos plots of DEmRNAs and DElncRNAs. (A) Heat map of the top 100 DEmRNAs between LUSC and normal tissues. Rows and columns represent DEmRNAs and tissue samples, respectively. Color scale indicates expression levels. (B) Heat map of the top 100 DElncRNAs between LUSC and normal tissues. Rows and columns represent DElncRNAs and tissue samples, respectively. Color scale indicates expression levels. (C) Circus plots represent the distribution of DElncRNAs and DEmRNAs on chromosomes. Red and blue colors represent upregulation and downregulation, respectively. DEmRNAs, differentially expressed mRNAs; DElncRNAs, differentially expressed long non-coding RNAs; LUSC, lung squamous cell carcinoma.

ROC curve analyses

As shown in *Figure 8*, *MCM2* (AUC =0.997), *SERPINB5* (AUC =0.979), *ITGB8* (AUC =0.913), *CASC19* (AUC =0.898), and *MIR205HG* (AUC =0.961) had a potential diagnostic value for LUSC except *NEAT1* (AUC =0.574).

Survival analysis

We assessed the prognostic value of 3 DEmRNAs (*MCM2*, *SERPINB5*, and *ITGB8*) and 3 DElncRNAs (*NEAT1*, *CASC19*, and *MIR205HG*) in LUSC. *SERPINB5*, *NEAT1*, and *MIR205HG* were found to be associated with the survival of LUSC patients (*Figure 9*).

MIR205HG knockdown inhibits NCI-H520 cell proliferation and migration

The lncRNA MIR205 host gene, *MIR205HG*, is a novel lncRNA involved in the regulation of various cancer cell processes. *MIR205HG* overexpression has been reported to be associated with tumor progression in esophageal cancer, ovarian cancer, and lung cancer (16-18). *MIR205HG* is associated with unlimited growth of head and neck squamous cell carcinoma cells (19). *MIR205HG*,

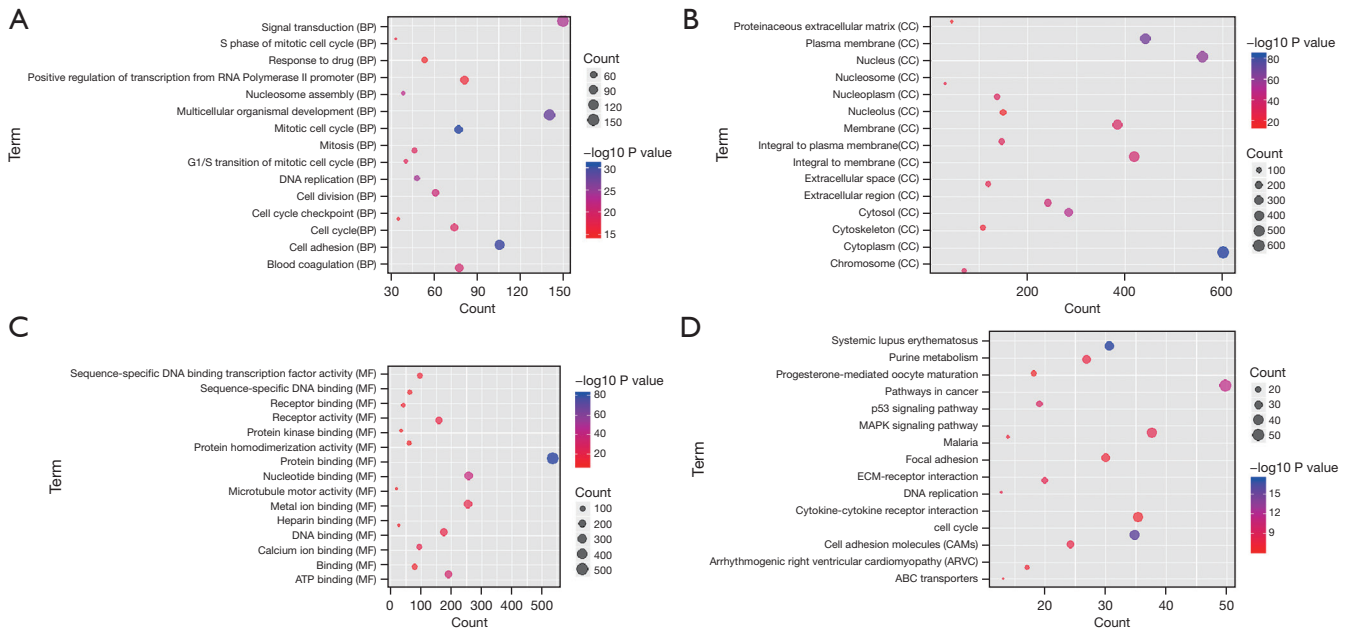

Figure 3 Top 15 significantly enriched GO terms and KEGG pathways for DEmRNAs in LUSC. (A) Biological process. (B) Cellular component. (C) Molecular function. (D) KEGG pathways. BP, biological process; CC, cellular component; MF, molecular function; GO, Gene Ontology; KEGG, Kyoto Encyclopedia of Genes and Genomes; DEmRNAs, differentially expressed mRNAs; LUSC, lung squamous cell carcinoma.

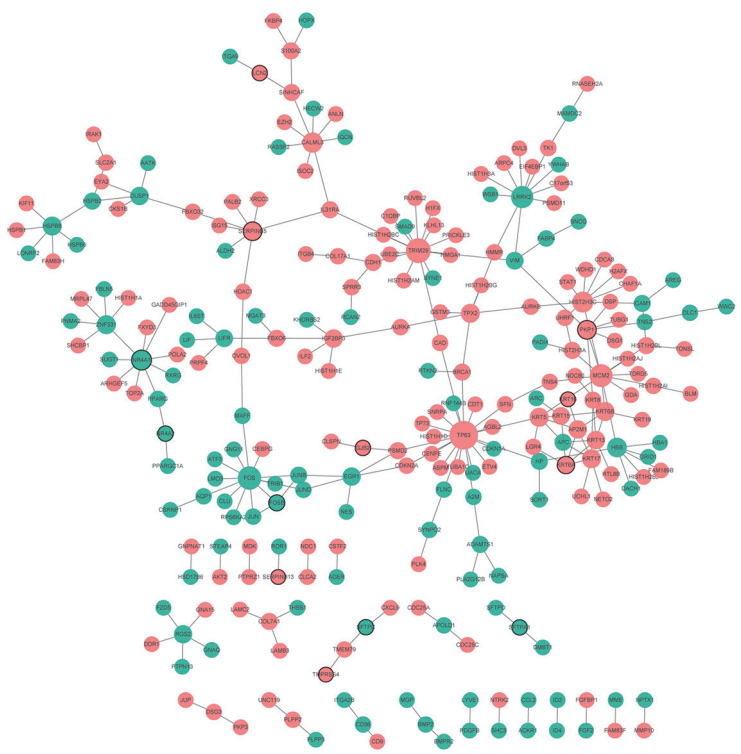

Figure 4 PPI network. Ellipses and lines represent nodes and edges, respectively. Red and green represent upward and downward adjustments, respectively. Black border indicates the top 10 upregulated and downregulated proteins. PPI, protein-protein interaction.

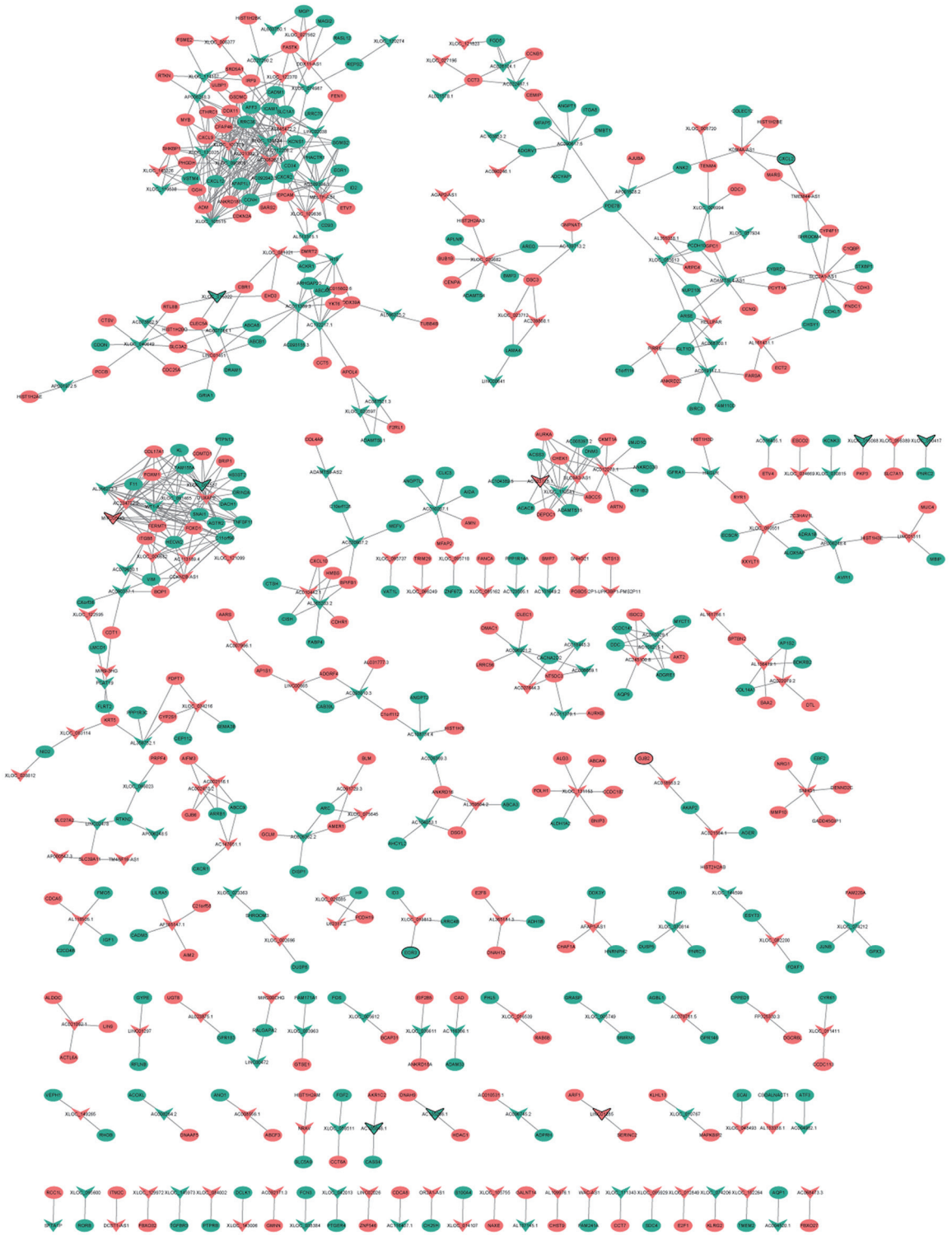

Figure 5 DEmRNAs and DElncRNAs co-expression in LUSC. Ellipses and rhombus represent DEmRNAs and DElncRNAs, respectively. Red and green colors represent upregulation and downregulation, respectively. Black border indicates the top 10 upregulated and downregulated DElncRNAs and DEmRNAs. DEmRNAs, differentially expressed mRNAs; DElncRNAs, differentially expressed long non-coding RNAs; LUSC, lung squamous cell carcinoma.

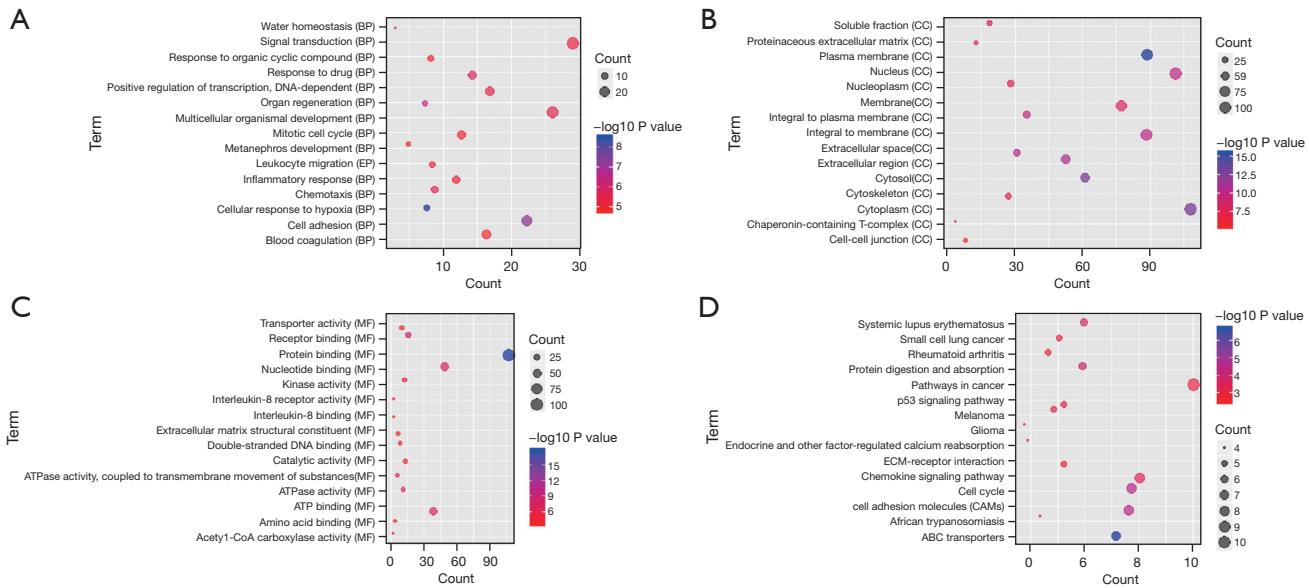

Figure 6 Top 15 significantly enriched GO terms and KEGG pathways for DEmRNAs co-expressed with DElncRNAs in LUSC. (A) Biological process. (B) Cellular component. (C) Molecular function, (D) KEGG pathways. BP, biological process; CC, cellular component; MF, molecular function; GO, Gene Ontology; KEGG, Kyoto Encyclopedia of Genes and Genomes; DEmRNAs, differentially expressed mRNAs; DElncRNAs, differentially expressed long non-coding RNAs; LUSC, lung squamous cell carcinoma.

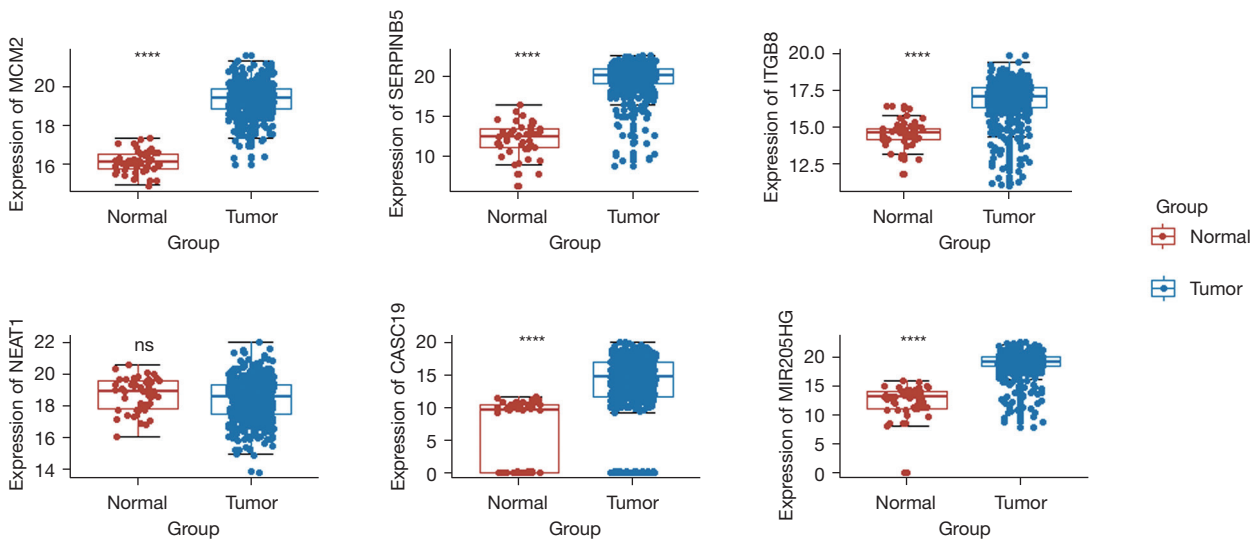

Figure 7 Expression validation in TCGA dataset. X-axis shows NCs (red) and LUSC (blue) groups. Y-axis shows a $\log_2$ transformation to the intensities. ****, P<0.0001; ns, not significant. TCGA, The Cancer Genome Atlas; NC, normal control; LUSC, lung squamous cell carcinoma.

as a competitive endogenous RNA, accelerates tumor proliferation and progression in cervical cancer by targeting miR-122-5p (20). *MIR205HG* regulates cell proliferation, apoptosis, and the migration of cervical cancer cells by modulating *SRSF1* and *KRT17* (21). In this study, we found that *MIR205HG* was co-expressed with *ITGB8* in LUSC. To further determine the effect of *MIR205HG* in LUSC, we used NCI-H520 cells to knock down MIR205HG. QRT-

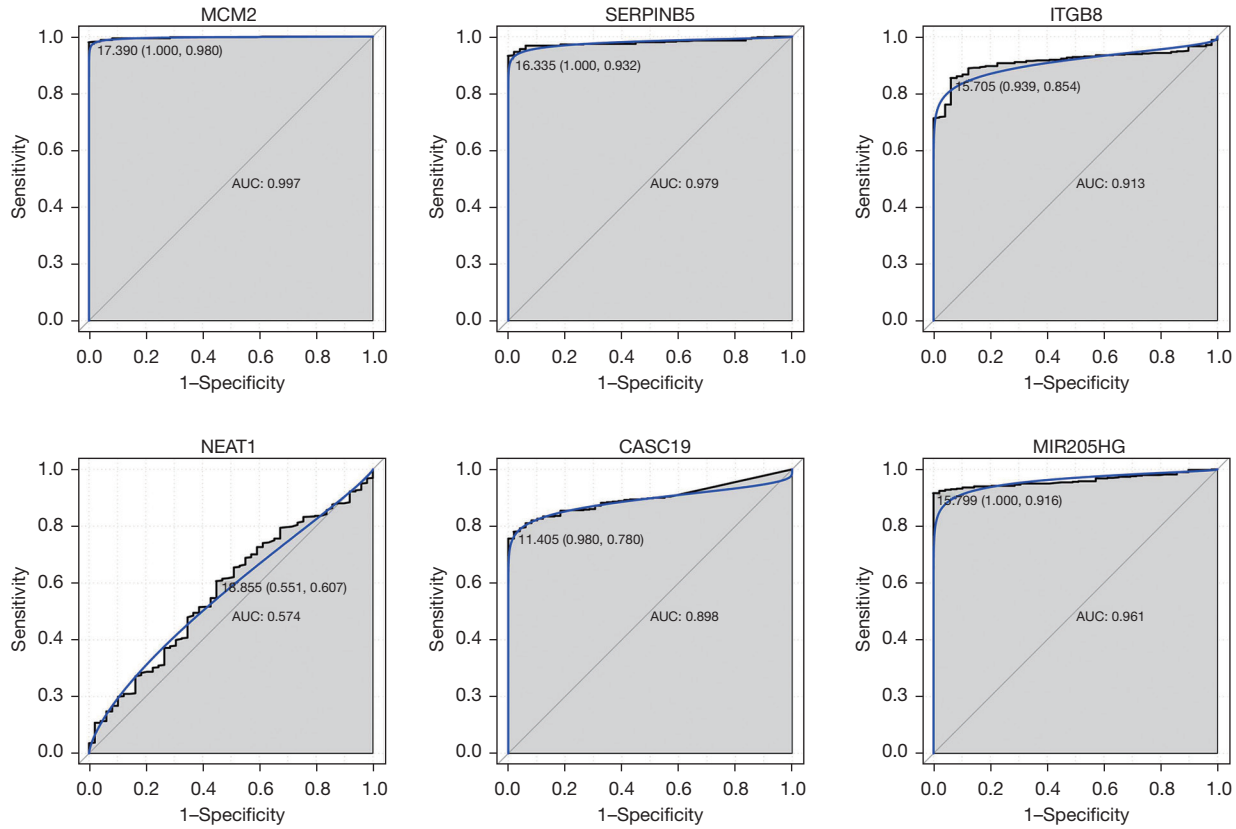

Figure 8 ROC curve analysis. X- and Y-axis indicate 1–specificity and sensitivity, respectively. AUC, area under the ROC curve; ROC, receiver-operating characteristic.

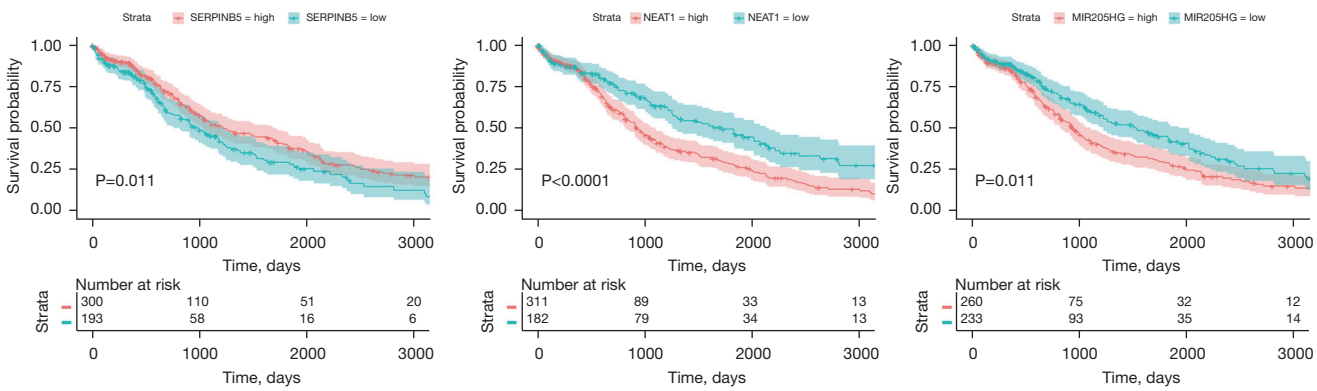

Figure 9 Survival analysis. X- and Y-axis show time (day) and survival rate of LUSC patients, respectively. LUSC, lung squamous cell carcinoma.

PCR was used to measure the relative mRNA expression of *MIR205HG* in NCI-H520 cells. As shown in *Figure 10A*, the expression of MIR205HG was markedly decreased in the si-*MIR205HG* group compared with the empty vector group. Then, 3-(4,5-dimetHylthiazol-2-yl)-2,5-diphenyltetrazolium bromide (MTT) assay and Transwell assay were used to detect the effect of *MIR205HG* on cell proliferation and migration, respectively. *MIR205HG* knockdown significantly inhibited the proliferation and migration of NCI-H520 cells (*Figure 10B,10C*). In

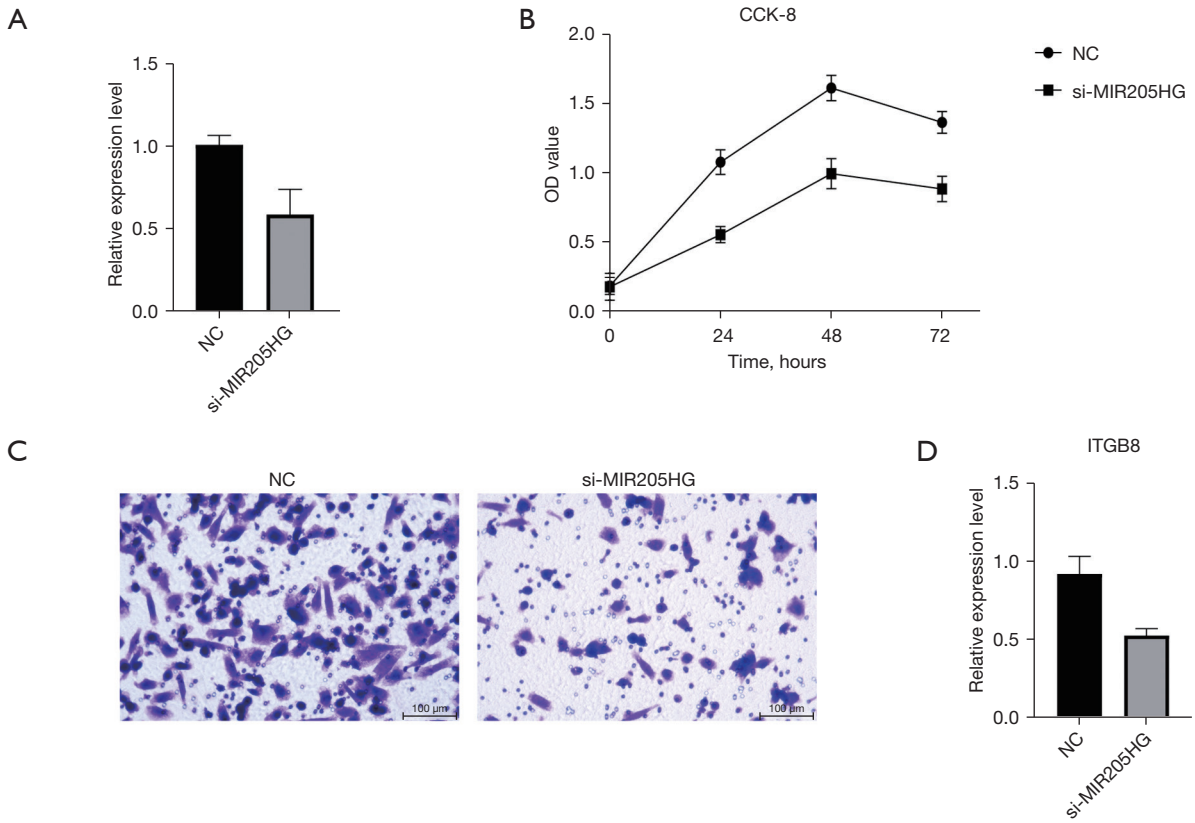

Figure 10 *MIR205HG* knockdown inhibits NCI-H520 cell proliferation and migration. (A) Transfection efficacy was detected by qRT-PCR. (B) MTT assay indicated that the viability of LUSC cells was suppressed by *MIR205HG* knockdown. (C) Transwell assay indicated that the migration ability of LUSC cells was inhibited by *MIR205HG* knockdown. Cells were stained with 0.25% crystal violet. (D) *ITGB8* expression was detected by qRT-PCR. NC, normal control; OD, optical density; CCK-8, Cell Counting Kit-8; qRT-PCR, quantitative reverse transcription polymerase chain reaction; MTT, 3-(4,5-dimethylthiazol-2-yl)-2,5-diphenyltetrazolium bromide; LUSC, lung squamous cell carcinoma.

addition, *MIR205HG* knockdown significantly reduced the expression of *ITGB8* (*Figure 10D*). These results indicate that *MIR205HG* knockdown could inhibit cell proliferation and migration in LUSC, and that *MIR205HG* could be a new target for the treatment of LUSC.

Discussion

Although the occurrence rate of LUSC is decreasing, it remains the highest cause of cancer-related morbidity (22). To date, RNA sequencing data analyses related to the expression profile of lncRNA in LUSC remain scarce (23). To determine the pathogenesis of LUSC, RNA sequencing was used to obtain DEmRNAs and DElncRNAs between LUSC and controls. It is a pity that there are not enough miRNAs to study competing endogenous RNA (ceRNA) (lncRNA-miRNA-mRNA) network. Therefore, we only focused on the mRNAs and lncRNAs in LUSC. A total of 1,946 DEmRNAs (940 downregulated and 1,006 upregulated mRNAs) and 428 DElncRNAs (206 downregulated and 222 upregulated lncRNAs) between LUSC and normal tissues were obtained. Functional annotation of DEmRNAs results showed that the cell cycle, cancer pathways, p53 signaling pathway, ECM-receptor interaction, DNA replication, and MAPK signaling pathway were significantly enriched pathways. PPI network and DEmRNA-DElncRNA interaction analyses were performed. Based on the functional annotation of DEmRNAs co-expressed with DElncRNAs, cell cycle, cell adhesion molecules, p53 signaling pathway, ECM-receptor interaction, small cell lung cancer, and focal adhesion were found to be significantly enriched pathways.

MCM2 belongs to the MCM family and has been identified as a biomarker for the progression and prognosis of several types of human cancers (24). *MCM2* is highly expressed in a variety of human cancers, including breast cancer, stomach cancer, colorectal cancer, lung cancer, and hepatocellular carcinoma (25-31). Wu *et al.* reported that the expression level of *MCM2* was upregulated in LUSC tissues and cell lines, and that *MCM2* was related to the low overall survival of LUSC patients (32). In this study, we performed RNA sequencing and found that *MCM2* expression was elevated between LUSC tissues and normal tissues. Based on the PPI network, *MCM2* was a hub protein in LUSC and was significantly enriched in the cell cycle pathway. Therefore, *MCM2* could be involved in the occurrence and development of LUSC by regulating the cell cycle pathway.

SERPINB5, a member of the serpin superfamily, is a serine protease inhibitor that suppresses tumor progression and metastasis (33-35). Higher *SERPINB5* expressions have been reported to be associated with better prognosis in non-small cell lung cancer, esophageal squamous cell carcinoma, ovarian cancer, and bladder cancer (25-27,36). In the present study, *SERPINB5* expression was increased in LUSC tissues compared with normal tissues. *SERPINB5*, a hub protein, was significantly enriched in the p53 signaling pathway. Isoalantolactone regulated cell cycle arrest and apoptosis of LUSC cells by activating the p53 signaling pathway (28). Therefore, *SERPINB5* could be involved in the occurrence and development of LUSC by regulating the p53 signaling pathway.

NEAT1 is a lncRNA that has been shown to be abnormally elevated in a variety of human cancers, such as lung cancer, oesophageal cancer, colorectal cancer and hepatocellular carcinoma (29). Recently, more and more studies have focused on *NEAT1*, which has been found to be involved in the occurrence and development of non-small cell lung cancer through targeting miRNAs and regulating multiple signaling pathways (30,31,37,38). *CASC19* is a novel lncRNA located on 8q24 region of the chromosome (39). *CASC19* has been reported to be increased in non-small cell lung cancer tissues and cell lines, and CASC19 accelerates cell proliferation, migration, and invasion of non-small cell lung cancer by regulating miRNA-130b-3p (40). In the present study, *NEAT1* and *CASC19* were also increased in LUSC tissues compared with normal tissues. In this study, we speculated that *NEAT1* and *CASC19* are involved the occurrence and development of LUSC.

The lncRNA MIR205 host gene, *MIR205HG*, is a novel lncRNA involved in the regulation of various cancer cell processes. *MIR205HG* overexpression has been reported to be associated with tumor progression in esophageal cancer, ovarian cancer, and lung cancer (16-18). *MIR205HG* is associated with unlimited growth of head and neck squamous cell carcinoma cells (19). *MIR205HG*, as a competitive endogenous RNA, accelerates tumor proliferation and progression in cervical cancer by targeting miR-122-5p (20). *MIR205HG* regulates cell proliferation, apoptosis, and the migration of cervical cancer cells by modulating *SRSF1* and *KRT17* (21). In the current study, *MIR205HG* was found to be increased in LUSC tissues compared with normal tissues. Through the DElncRNA-DEmRNA interaction network, *ITGB8* was found to be co-expressed with *MIR205HG*. *ITGB8* was significantly enriched in ECM-receptor interaction, cell adhesion molecules, and focal adhesion. In our study, *MIR205HG* knockdown was found to inhibit cell proliferation and migration in LUSC, and significantly reduced the expression of *ITGB8*. These findings indicated that *MIR205HG* inhibits LUSC cell proliferation and migration by modulating *ITGB8* expression.

The present study had some limitations. More samples were needed to validate the expression of mRNAs and lncRNAs. Furthermore, further *in vivo* and *in vitro* experiments are warranted to determine the biological functions of representative downregulated lncRNAs in LUSC.

In conclusion, we identified 1,946 DEmRNAs and 428 DElncRNAs in LUSC compared with normal tissues. Cell cycle, cancer pathways, the p53 signaling pathway, ECM-receptor interaction, DNA replication, and the MAPK signaling pathway were found to be significantly enriched pathways of DEmRNAs. Based on the PPI network, *TP63*, *TRIM29*, *FOS*, *MCM2*, *LRRK2*, *NR4A1*, *HIST2H3C*, *CALML3*, *HBB*, *PKP1*, and *SERPINB5* were considered to be hub proteins. In total, 851 DElncRNA-DEmRNA co-expression pairs were obtained. Cell cycle, cell adhesion molecules, p53 signaling pathway, ECM-receptor interaction, small cell lung cancer and focal adhesion were found to be significantly enriched pathways of DEmRNAs co-expressed with DElncRNAs. ROC curve analysis indicated that *MCM2*, *SERPINB5*, *ITGB8*, *CASC19*, and *MIR205HG* could predict the occurrence of LUSC. Survival analysis suggested that *SERPINB5*, *NEAT1*, and *MIR205HG* had potential prognostic value for LUSC. This finding could help determine the mechanisms and potential treatment targets of LUSC.

Acknowledgments

Funding: None.

Footnote

Reporting Checklist: The authors have completed the STARD and MDAR reporting checklists. Available at https://jtd.amegroups.com/article/view/10.21037/jtd-22-343/rc

Data Sharing Statement: Available at https://jtd.amegroups.com/article/view/10.21037/jtd-22-343/dss

Conflicts of Interest: All authors have completed the ICMJE uniform disclosure form (available at https://jtd.amegroups.com/article/view/10.21037/jtd-22-343/coif). The authors have no conflicts of interest to declare.

Ethical Statement: The authors are accountable for all aspects of the work in ensuring that questions related to the accuracy or integrity of any part of the work are appropriately investigated and resolved. The study was conducted in accordance with the Declaration of Helsinki (as revised in 2013). This study was approved by the ethics committee of the Fourth Hospital of Hebei Medical University (No. 2019KY256). Written informed consent was obtained from all participants.

References

1. Zhang Y, Simoff MJ, Ost D, et al. Understanding the patient journey to diagnosis of lung cancer. BMC Cancer 2021;21:402.
2. Bi H, Ren D, Wu J, et al. Lung squamous cell carcinoma with rare epidermal growth factor receptor mutation G719X: a case report and literature review. Ann Transl Med 2021;9:1805.
3. Wang Z, Wang Z, Niu X, et al. Identification of seven-gene signature for prediction of lung squamous cell carcinoma. Onco Targets Ther 2019;12:5979-88.
4. Guo T, Li J, Zhang L, et al. Multidimensional communication of microRNAs and long non-coding RNAs in lung cancer. J Cancer Res Clin Oncol 2019;145:31-48.
5. Choi M, Kadara H, Zhang J, et al. Mutation profiles in early-stage lung squamous cell carcinoma with clinical follow-up and correlation with markers of immune function. Ann Oncol 2017;28:83-9.
6. Liu Y, Liu B, Jin G, et al. An Integrated Three-Long Non-coding RNA Signature Predicts Prognosis in Colorectal Cancer Patients. Front Oncol 2019;9:1269.
7. Zhao Y, Zhang Y, Zhang L, et al. The Potential Markers of Circulating microRNAs and long non-coding RNAs in Alzheimer's Disease. Aging Dis 2019;10:1293-301.
8. Wang Y, Wu N, Liu J, et al. FusionCancer: a database of cancer fusion genes derived from RNA-seq data. Diagn Pathol 2015;10:131.
9. Jiao Y, Li Y, Ji B, et al. Clinical Value of lncRNA LUCAT1 Expression in Liver Cancer and its Potential Pathways. J Gastrointestin Liver Dis 2019;28:439-47.
10. Kim N, Kim HK, Lee K, et al. Single-cell RNA sequencing demonstrates the molecular and cellular reprogramming of metastatic lung adenocarcinoma. Nat Commun 2020;11:2285.
11. Chen S, Liu Y, Wang Y, et al. LncRNA CCAT1 Promotes Colorectal Cancer Tumorigenesis Via A miR-181b-5p/TUSC3 Axis. Onco Targets Ther 2019;12:9215-25.
12. Robinson MD, McCarthy DJ, Smyth GK. edgeR: a Bioconductor package for differential expression analysis of digital gene expression data. Bioinformatics 2010;26:139-40.
13. Still BR, Christianson LW, Mhlaba JM, et al. Standardization of Disposable Instruments in Microvascular Breast Reconstruction: A Case Study in Cost Reduction. J Reconstr Microsurg 2017;33:92-6.
14. Tabas-Madrid D, Nogales-Cadenas R, Pascual-Montano A. GeneCodis3: a non-redundant and modular enrichment analysis tool for functional genomics. Nucleic Acids Res 2012;40:W478-83.
15. Robin X, Turck N, Hainard A, et al. pROC: an open-source package for R and S+ to analyze and compare ROC curves. BMC Bioinformatics 2011;12:77.
16. Iorio MV, Visone R, Di Leva G, et al. MicroRNA signatures in human ovarian cancer. Cancer Res 2007;67:8699-707.
17. Hezova R, Kovarikova A, Srovnal J, et al. MiR-205 functions as a tumor suppressor in adenocarcinoma and an oncogene in squamous cell carcinoma of esophagus. Tumour Biol 2016;37:8007-18.

18. Zarogoulidis P, Petanidis S, Kioseoglou E, et al. MiR-205 and miR-218 expression is associated with carboplatin chemoresistance and regulation of apoptosis via Mcl-1 and Survivin in lung cancer cells. Cell Signal 2015;27:1576-88.
19. Di Agostino S, Valenti F, Sacconi A, et al. Long Non-coding MIR205HG Depletes Hsa-miR-590-3p Leading to Unrestrained Proliferation in Head and Neck Squamous Cell Carcinoma. Theranostics 2018;8:1850-68.
20. Li Y, Wang H, Huang H. Long non-coding RNA MIR205HG function as a ceRNA to accelerate tumor growth and progression via sponging miR-122-5p in cervical cancer. Biochem Biophys Res Commun 2019;514:78-85.
21. Dong M, Dong Z, Zhu X, et al. Long non-coding RNA MIR205HG regulates KRT17 and tumor processes in cervical cancer via interaction with SRSF1. Exp Mol Pathol 2019;111:104322.
22. Ferlay J, Soerjomataram I, Dikshit R, et al. Cancer incidence and mortality worldwide: sources, methods and major patterns in GLOBOCAN 2012. Int J Cancer 2015;136:E359-86.
23. Li R, Yang YE, Jin J, et al. Identification of lncRNA biomarkers in lung squamous cell carcinoma using comprehensive analysis of lncRNA mediated ceRNA network. Artif Cells Nanomed Biotechnol 2019;47:3246-58.
24. Del Moral-Hernández O, Hernández-Sotelo D, Alarcón-Romero LDC, et al. TOP2A/MCM2, p16INK4a, and cyclin E1 expression in liquid-based cytology: a biomarkers panel for progression risk of cervical premalignant lesions. BMC Cancer 2021;21:39.
25. Wang Y, Sheng S, Zhang J, et al. Elevated maspin expression is associated with better overall survival in esophageal squamous cell carcinoma (ESCC). PLoS One 2013;8:e63581.
26. Takanami I, Abiko T, Koizumi S. Expression of maspin in non-small-cell lung cancer: correlation with clinical features. Clin Lung Cancer 2008;9:361-6.
27. Kramer MW, Waalkes S, Hennenlotter J, et al. Maspin protein expression correlates with tumor progression in non-muscle invasive bladder cancer. Oncol Lett 2010;1:621-6.
28. Jin C, Zhang G, Zhang Y, et al. Isoalantolactone induces intrinsic apoptosis through p53 signaling pathway in human lung squamous carcinoma cells. PLoS One 2017;12:e0181731.
29. Yu X, Li Z, Zheng H, et al. NEAT1: A novel cancer-related long non-coding RNA. Cell Prolif 2017;50:e12329.
30. Sun C, Li S, Zhang F, et al. Long non-coding RNA NEAT1 promotes non-small cell lung cancer progression through regulation of miR-377-3p-E2F3 pathway. Oncotarget 2016;7:51784-814.
31. Sun SJ, Lin Q, Ma JX, et al. Long non-coding RNA NEAT1 acts as oncogene in NSCLC by regulating the Wnt signaling pathway. Eur Rev Med Pharmacol Sci 2017;21:504-10.
32. Wu W, Wang X, Shan C, et al. Minichromosome maintenance protein 2 correlates with the malignant status and regulates proliferation and cell cycle in lung squamous cell carcinoma. Onco Targets Ther 2018;11:5025-34.
33. Kisling SG, Natarajan G, Pothuraju R, et al. Implications of prognosis-associated genes in pancreatic tumor metastasis: lessons from global studies in bioinformatics. Cancer Metastasis Rev 2021;40:721-38.
34. D'Aguanno S, Mallone F, Marenco M, et al. Hypoxia-dependent drivers of melanoma progression. J Exp Clin Cancer Res 2021;40:159.
35. Drew J, Machesky LM. The liver metastatic niche: modelling the extracellular matrix in metastasis. Dis Model Mech 2021;14:dmm048801.
36. Klasa-Mazurkiewicz D, Narkiewicz J, Milczek T, et al. Maspin overexpression correlates with positive response to primary chemotherapy in ovarian cancer patients. Gynecol Oncol 2009;113:91-8.
37. Li S, Yang J, Xia Y, et al. Long Noncoding RNA NEAT1 Promotes Proliferation and Invasion via Targeting miR-181a-5p in Non-Small Cell Lung Cancer. Oncol Res 2018;26:289-96.
38. Jiang P, Chen A, Wu X, et al. NEAT1 acts as an inducer of cancer stem cell-like phenotypes in NSCLC by inhibiting EGCG-upregulated CTR1. J Cell Physiol 2018;233:4852-63.
39. Teerlink CC, Leongamornlert D, Dadaev T, et al. Genome-wide association of familial prostate cancer cases identifies evidence for a rare segregating haplotype at 8q24.21. Hum Genet 2016;135:923-38.
40. Qu CX, Shi XC, Zai LQ, et al. LncRNA CASC19 promotes the proliferation, migration and invasion of non-small cell lung carcinoma via regulating miRNA-130b-3p. Eur Rev Med Pharmacol Sci 2019;23:247-55.

Cite this article as: Zhao X, Yuan C, He X, Wang M, Zhang H, Cheng J, Wang H. Identification and *in vitro* validation of diagnostic and prognostic biomarkers for lung squamous cell carcinoma. J Thorac Dis 2022;14(4):1243-1255. doi: 10.21037/jtd-22-343